Molecular Vision 2016; 22:718-733 <http://www.molvis.org/molvis/v22/718>
Received 11 March 2016 | Accepted 22 June 2016 | Published 24 June 2016

An ex vivo gene therapy approach in X-linked retinoschisis

Abu E. Bashar, Andrew L. Metcalfe, Ishaq A. Viringipurampeer, Anat Yanai, Cheryl Y. Gregory-Evans, Kevin Gregory-Evans

Department of Ophthalmology, University of British Columbia, Vancouver BC, Canada

Purpose: X-linked retinoschisis (XLRS) is juvenile-onset macular degeneration caused by haploinsufficiency of the extracellular cell adhesion protein retinoschisin (RS1). *RS1* mutations can lead to either a non-functional protein or the absence of protein secretion, and it has been established that extracellular deficiency of RS1 is the underlying cause of the phenotype. Therefore, we hypothesized that an ex vivo gene therapy strategy could be used to deliver sufficient extracellular RS1 to reverse the phenotype seen in XLRS. Here, we used adipose-derived, syngeneic mesenchymal stem cells (MSCs) that were genetically modified to secrete human RS1 and then delivered these cells by intravitreal injection to the retina of the *Rs1h* knockout mouse model of XLRS.

Methods: MSCs were electroporated with two transgene expression systems (cytomegalovirus (CMV)-controlled constitutive and doxycycline-induced Tet-On controlled inducible), both driving expression of human *RS1* cDNA. The stably transfected cells, using either constitutive mesenchymal stem cell (MSC) or inducible MSC cassettes, were assayed for their RS1 secretion profile. For single injection studies, 100,000 genetically modified MSCs were injected into the vitreous cavity of the *Rs1h* knockout mouse eye at P21, and data were recorded at 2, 4, and 8 weeks post-injection. The control groups received either unmodified MSCs or vehicle injection. For the multiple injection studies, the mice received intravitreal MSC injections at P21, P60, and P90 with data collection at P120. For the single- and multiple-injection studies, the outcomes were measured with electroretinography, optokinetic tracking responses (OKT), histology, and immunohistochemistry.

Results: Two lines of genetically modified MSCs were established and found to secrete RS1 at a rate of 8 ng/million cells/day. Following intravitreal injection, RS1-expressing MSCs were found mainly in the inner retinal layers. Two weeks after a single injection of MSCs, the area of the schisis cavities was reduced by 65% with constitutive MSCs and by 83% with inducible MSCs, demonstrating improved inner nuclear layer architecture. This benefit was maintained up to 8 weeks post-injection and corresponded to a significant improvement in the electroretinogram (ERG) b-/a-wave ratio at 8 weeks (2.6 inducible MSCs; 1.4 untreated eyes, $p<0.05$). At 4 months after multiple injections, the schisis cavity areas were reduced by 78% for inducible MSCs and constitutive MSCs, more photoreceptor nuclei were present (700/µm constitutive MSC; 750/µm inducible MSC; 383/µm untreated), and the ERG b-wave was significantly improved (threefold higher with constitutive MSCs and twofold higher with inducible MSCs) compared to the untreated control group.

Conclusions: These results establish that extracellular delivery of RS1 rescues the structural and functional deficits in the *Rs1h* knockout mouse model and that this ex vivo gene therapy approach can inhibit progression of disease. This proof-of-principle work suggests that other inherited retinal degenerations caused by a deficiency of extracellular matrix proteins could be targeted by this strategy.

With a prevalence of 1:5,000 to 1:25,000, X-linked retinoschisis (XLRS) is one of the most common causes of retinal disease and blindness in young men [1]. The disease is caused by more than 180 mutations in the *retinoschisin* (*RS1*; Gene ID: 6247; OMIM 300839) gene localized to Xp22.13 [2,3]. The RS1 protein is expressed and secreted by retinal photoreceptors and bipolar cells [4] and functions as a cell adhesion molecule between the photoreceptors and the bipolar cells [5]. Absence or non-functional expression of RS1 protein results in significant and progressive structural abnormalities in the outer and inner retina described as schisis cavities with accompanying progressive death of the photoreceptor cells [2].

Several preclinical in vivo gene therapy studies have reported positive benefits in animal models of XLRS [6-9]. To date, however, these models suffered from the limitations inherent in many current in vivo gene therapy protocols: lack of specificity, low efficiency, and systemic exposure to the transport vector [10-13]. An ex vivo approach to gene therapy could circumvent many of these issues. XLRS is a good candidate for ex vivo gene therapy for three reasons: First, it is a monogenic disorder where the underlying pathophysiology is well understood. Second, gene therapy techniques to improve wild-type protein production are best suited to loss-of-protein phenotypes such as in XLRS instead of in gain-of-function mutations where pathophysiology has been linked to the adverse effects of a mutant protein. Third, RS1

Correspondence to: Kevin Gregory-Evans, Department of Ophthalmology, University of British Columbia, Eye Care Centre, 2550 Willow Street, Vancouver, BC, V5Z 3N9, Canada; Phone: (604)-875-5275; FAX: (604) 875-4663; email: kge30@mail.ubc.ca

is a secreted, extracellular protein, so it can be replaced in the retinal extracellular space by secretion from other cell types (e.g., mesenchymal stem cells [MSCs]).

MSCs are multipotent non-hematopoietic stromal cells found within many tissues. Interest in the therapeutic potential of MSCs was originally focused on their tissue regenerative properties. More recently, their paracrine effects, in terms of neurotrophic and immunomodulatory abilities, have become increasingly recognized [14]. MSCs are known to protect injured neurons, stimulate angiogenesis in stroke, promote wound healing, and inhibit fibrosis through their paracrine effectors [15]. In addition, their remarkable homing ability allows MSCs to migrate into areas of tissue damage and integrate into the tissues' extracellular compartment [15]. Mesenchymal stem cells have been used in several cell-based therapeutic studies to treat retinal degeneration [16-20]. It has yet to be assessed whether the paracrine effects of MSCs can be combined with the expression of novel proteins through an ex vivo gene therapy approach. Another particular advantage of an ex vivo protocol is the relative ease with which cells can be engineered to vary the expression of novel proteins in response to external signals. The Tet-On system is a well-known molecular switch used for this purpose, where expression can be induced by exposure to doxycycline [21].

In this study, we tested an ex vivo gene therapy approach in the *Rs1h* mouse model of XLRS. MSCs that either expressed human *RS1* constitutively (constitutive MSCs) or inducibly (inducible MSCs) were delivered into the mouse eye by intravitreal injection. Efficacy of the therapy was assessed with measurements of the histological and functional outcomes.

METHODS

Disease model: Homozygous female *Rs1h* knockout (KO) and hemizygous male *Rs1h* KO animals were obtained from the laboratories of Dr. R. Molday (University of British Columbia). Offspring were genotyped with PCR to verify the genetic status using two sets of primers. PCR conditions: Denaturation - 30 s, 94 ºC. Annealing - 30 s at 60 ºC; Extension - 45 s at 72 ºC. Final extension cycle extended to 10 min at 72 ºC. Cycles repeated 35 times.One set (forward: 5′-TGA GGA CCC CTG GTA CCA GAA-3′; reverse: 5′-CCA TCT CAG GCA AGC CAG G-3′) was designed to amplify a 260 bp region of the wild-type *Rsh1* gene. The same forward primer was used in combination with a different reverse primer targeting LacZ (5′-CAA GGC GAT TAA GTT GGG TAA C-3′) to detect the mutant *Rs1h* gene (product size 180 bp) [22]. Homozygous female and hemizygous male offspring were used for this study. The animals were housed under standard conditions (25 °C; 10% relative humidity, and a 12-h:12 h light-dark cycle) and had free access to food and water throughout the experiment. These studies were approved by the University of British Columbia Animal Care Committee in Canada and were performed in accordance with the ARVO Statement for the Use of Animals in Ophthalmic and Vision Research.

Cloning of RS1 cDNA: For the constitutive expression cassette, the human *RS1* cDNA (gift from Dr. R. Molday) was cloned into the pIRES2-DsRed2 vector (Clontech, Mountain View, CA) driven by a constitutive cytomegalovirus (CMV) promoter. This plasmid also carries the neomycin-resistance gene for the selection of transfected cells with the antibiotic Geneticin (G418). This plasmid was used to transform competent DH5α *E. coli* cells (New England Biolabs, Whitby, Canada). The transformed bacterial cells were cultured overnight at 37 °C in Luria Broth media (Thermo Fisher Scientific, Ottawa, Canada) containing 50 µg/ml kanamycin (Thermo Fisher Scientific). Plasmid isolation was performed using the PureYield™ Plasmid Maxiprep System (Promega, Madison, WI) according to the manufacturer's instructions. The presence of the *RS1* cDNA in the plasmid was confirmed by restriction digestion and subsequent 1% agarose gel electrophoresis.

For the inducible expression cassette, a Tet-On system (Clontech) was used that contained two plasmids: pTRE3G-BI-mCherry and pCMV-Tet3G. The human *RS1* cDNA was cloned into the pTRE3G-BI-mCherry vector. This plasmid system carries the hygromycin-resistance gene for the selection of transfected cells with the antibiotic Hygromycin (Hyg). The other plasmid (pCMV-Tet3G) carries the neomycin-resistance gene for the selection of transfected cells with the antibiotic Geneticin (G418). Both plasmids were amplified using DH5α *E. coli* cells following the above-described procedure. The presence of *RS1* cDNA in the pTRE3G-BI-mCherry plasmid was confirmed by restriction digestion and gel electrophoresis.

Cell culture: MSCs were isolated from inguinal adipose tissue (AMSCs) as previously described [14]. Briefly, the tissue from P21 C57BL/6J mice was macerated with surgical scissors in 3 ml of 1 mg/ml Collagenase I (Sigma-Aldrich, Oakville, Canada) in Dulbecco's PBS (Life Technologies, Burlington, Canada) and incubated at 37 °C for 1 h. Collagenase-dissociated tissue was filtered through a sterile 40 µm cell strainer (Stemcell Technologies, Vancouver, Canada) into a 50 ml sterile tube and centrifuged at 1,000 ×*g* for 10 min. The supernatant was removed, and the cell pellet was resuspended in MesenCult MSC Basal Medium (Stemcell Technologies) supplemented with 15% heat-inactivated fetal

bovine serum and 1% penicillin/streptomycin (both from Life Technologies). The cells were plated in a six-well dish and allowed to adhere for 48 h in a 37 °C incubator with 5% CO_2. Upon reaching confluency, the cells were passaged to a T-75 cell culture flask as previously described [14].

WeriRB human retinoblastoma (Weri-Rb-1) cells were obtained from American Type Culture Collection (Manassas, VA). These cells were used after two passages as a control to show the size of the human RS1 protein on western blot as previously authenticated [23]. The cells were thawed and maintained in suspension culture in RPMI 1640 media (Life Technologies) supplemented with 10% heat-inactivated fetal bovine serum (Life Technologies) and 1% penicillin/streptomycin (Life Technologies). The cells were plated in a T-75 cell culture flask and incubated in a 37 °C incubator with 5% CO_2.

MSC transfection with RS1 cDNA containing expression vector: Mouse MSCs were electroporated using the Gene Pulser Xcell system (Bio-Rad, Mississauga, Canada). Briefly, MSCs from an early passage (3–5) were dissociated with 0.05% Trypsin-EDTA (Life Technologies), counted, and collected by centrifugation. One million cells were resuspended in 500 µl of Gene Pulser electroporation buffer (Bio-Rad) and transferred into a 0.4 cm electroporation cuvette (Bio-Rad). For the constitutive expression, 100 µl pIRES2-DsRed2-RS1 plasmid (1 µg/µl) was mixed thoroughly with the MSCs containing electroporation buffer. A square wave pulse of 220 V for 25 msec was applied to the cells, which were then quickly plated in a six-well dish with 2 ml MesenCult MSC Basal Medium and incubated at 37 °C. The medium was replaced 24 h later with MSC media containing 200 µg/ml G418 (Geneticin, Life Technologies) for selection over a 2-week period. Transfection was confirmed by visualization of the reporter gene DsRed2, using a Zeiss LSM 510 META confocal laser scanning system (Zeiss Canada, Toronto, Canada).

Expression and secretion of RS1 from transfected cells were assessed with an enzyme-linked immunosorbent assay (ELISA) as described previously [14]. Briefly, 1,000 transfected cells in 200 µl of culture media were plated into a 24-well tissue culture dish. Five days later, the media were collected from each well, and the cells were lysed with 200 µl of lysis buffer (10 mM Tris-HCl pH 7.4, 2 mM EDTA, 150 mM NaCl, 0.875% Brij-96, 0.125% NP-40, 1 µg/ml aprotinin, 1 µg/ml leupeptin, and 174 µg/ml phenylmethane sulfonyl fluoride [PMSF]). Lysates were collected in 0.5 ml tubes and were subjected to three freeze–thaw cycles. After brief centrifugation for 1 min at 10,000 ×*g*, the supernatant was collected. Using 100 µl of cell lysate or media, RS1 expression and secretion were measured using ELISA kit (USCN Life Sciences Inc., Wuhan, China) following the manufacturer's instructions. Visualization of the chromogenic substrates was measured at 450 nm using a POLARstar Omega plate reader (BMG LABTECH, GmbH, Ortenberg, Germany). All samples were analyzed in duplicate (n = 3), and the results were calculated as ng/million cells/day.

For the inducible system, two rounds of transfection were performed. First, 100 µl of pCMV-Tet3G (1 µg/µl) plasmid was used to transfect the mouse MSCs. Successfully transfected cells (TetMSCs were selected using G418 (200 µg/ml) for 2 weeks followed by rapid expansion. A second round of transfection was performed using the pTRE3G-BI-mCherry vector with *RS1* cDNA (1 µg/µl) on the TetMSCs following a similar electroporation process. Transiently transfected cells were observed by imaging the reporter gene mCherry using confocal imaging. Hygromycin (Thermo Fisher Scientific) selection media (200 µg/ml) were used to select the transfected cells (inducible MSCs) for 2 weeks, and then RS1 secretion was measured as described above.

Intravitreal injection: For the single-injection protocol, expanded AMSCs, constitutive MSCs, and inducible MSCs were resuspended in Dulbecco's PBS (ThermoFisher Scientific, Product No: 14190250, Burlingham, Canada) to give a final concentration of 50,000 cells/µl. A 30 gauge needle was used with the Hamilton was used to inject 2 µl of the cell suspension (1×10^5 cells) into the vitreous cavity of the left eye of the P21 *Rs1h* mice. The injection site was about 1 mm behind the limbus. The animals were anesthetized by inhalation using 3% isoflurane. Five groups of animals received constitutive RS1-secreting MSCs, inducible RS1-secreting MSCs, unmodified AMSCs, or culture media (vehicle) or were untreated. Immunosuppression was not used in any animals. Data were collected at 2-, 4-, and 8-week post-injection time points. For the multiple injection protocol, the first injection was performed at P30, followed by injections at P60 and P90. There were three cohorts in this study: inducible MSCs, constitutive MSCs, and untreated. Data were collected at P120.

Topical doxycycline administration: To test the penetration of doxycycline into the retina, *Rs1h* mice (n = 3) were treated with topical Doxycycline Hyclate (doxycycline; Sigma-Aldrich) for 7 consecutive days. Two concentrations of doxycycline were prepared (5 and 10 mg/ml) using PBS (Life Technologies). Doxycycline (50 µl) was applied to the left eye of each animal using a dropper. For the in vivo studies (intravitreal inducible MSCs), 50 µl of 5 mg/ml doxycycline was topically administered to all animals 1 day after the injection and continued once daily until the sampling date.

Electroretinography: Mice were dark-adapted overnight, then anesthetized with an intraperitoneal injection of xylazine (16 mg/kg) and ketamine (120 mg/kg), and maintained on a heating pad. Using topical 0.5% proparacaine hydrochloride (Bausch and Lomb, Rochester, NY), the cornea was anesthetized, and the pupils were dilated with 2.5% phenylephrine and 1% atropine. A drop of 2% hydroxy-propyl-methyl-cellulose was placed on each cornea to keep it moist. Electroretinograms (ERGs) were recorded using an Espion V5 Electroretinography Console plus ColorDome Mini-Ganzfeld stimulator (Diagnosys LLC, Lowell, MA) with corneal contact lens electrodes. Scotopic ERGs (reflecting rod function) were recorded using white flashes of intensity 2.25 cd.s/m^2. Photopic ERGs (mixed rod and cone function) were recorded with the background illumination set at 30 cd/m^2 and white flashes of 3.0 cd.s/m^2. The average scotopic b-/a-wave ratio was calculated. The sample size was six for all cohorts for the single- and multiple-injection studies.

Optokinetic tracking: To examine visually driven behavioral responses, optokinetic tracking (OKT) was used to measure the spatial frequency thresholds under photopic (light-adapted) conditions [24]. A vertical sine wave grating (100% contrast) was projected as a virtual cylinder in three-dimensional space on computer monitors arranged in a quadrangle around a testing arena (OptoMotry; CerebralMechanics, Lethbridge, Canada). Unrestrained mice were placed on the elevated platform at the center of the equipment. An observer used a video monitor to ensure that the virtual cylinder was kept centered on the animal's head and recorded head movements in response to cylinder rotation. The highest spatial frequency that resulted in a head movement response was documented. The sample size was six for all cohorts for the single- and multiple-injection studies.

Histology: Animals were euthanized with CO_2 asphyxiation. The eyes were enucleated and marked at the 12 o'clock position, by leaving a piece of white conjunctiva muscle for orientation. The eyes were immersed in 50% Karnovsky fixative for 1 h, and the anterior segment was removed by excision at the ora serrata. The posterior eyecups were embedded in paraffin, cut sagittally to a thickness of 5 µm, and counterstained with hematoxylin and eosin. Schisis cavities within the inner nuclear layer were analyzed. To standardize the schisis area measurement of different eyes, only sagittal sections that included the optic nerve were assessed. Images were overlaid with a 200-µm-long rectangular template using Adobe Photoshop CS2. This template was positioned at four predetermined coordinates to give counts from two central (behind the equator) and two peripheral (in front of the equator) coordinates as previously described [25]. These four images for each eye were then imported into ImageJ (v 1.37), converted to grayscale, and inverted, and the schisis areas were measured by saturating the black areas. For the multiple-injection study, the same four 200 µm areas were used to count the outer nuclear layer cell number. The sample size was six for all the cohorts for single- and multiple-injection studies.

ELISA: Retinal lysates were analyzed with ELISA to detect RS1 expression following the previously described protocol [16,26]. Briefly, isolated neurosensory retinas from mouse eyes were collected and homogenized with a 25G needle using 200 µl cold PBS. Homogenates were then centrifuged for 10 min at 13,000 ×*g*, and the protein concentration was then determined with the Bradford (Bio-Rad Protein Assay) method in the cleared supernatants. RS1 concentrations were measured using a sandwich ELISA (USCN Life Science Inc.) according to the manufacturer's instruction [14] and visualized as described for MSCs. All samples were analyzed in duplicate, and the results were calculated as pg/100 mg. For all data, the sample size was three.

Immunohistochemistry: Eyes were enucleated from three mice cohorts (constitutive MSCs, inducible MSCs, and untreated) for single and multiple injections, fixed in 4% paraformaldehyde (PFA, EMS, Hatfield, PA) overnight, and subsequently incubated in 25% (W/V) sucrose for 24 h. The eyes were embedded in Tissue-Tek Cryomolds (Sakura Finetek USA Inc., Torrance, CA) with PolyFreeze Tissue Freezing Medium (Polysciences, Inc., Warrington, PA). Ten-micron-thick sections were cut using a Microm HM 525 microtome (Thermo Fisher, Waltham, MA). Sections were stained to locate MSCs and track RS1 expression. Although tracking MSCs in vivo has been a challenge [27], recent studies showed that PDGF receptor alpha (PDGFRα) can be used for in vitro and in vivo tracking [28]. Immunostaining was performed following established protocols [25]. Briefly, the cryosections were blocked with PBS containing 0.2% Triton X-100 (PBS-T) and 10% (v/v) goat serum for 1 h and labeled overnight with a primary rabbit polyclonal RS1 antibody (1:1,000; gift from Dr. Molday, UBC) and a polyclonal goat PDGFRα antibody (1:50; R&D, Minneapolis, MN). The samples were then rinsed in PBS and labeled for 1 h with secondary antibodies: a goat anti-rabbit immunoglobulin (IgG) conjugated to Alexa Fluor 594 (Life Technologies) for the polyclonal RS1 antibody and donkey anti-goat IgG conjugated to DyLight 488 (Thermo Fisher) for the polyclonal PDGFRα antibody.

Statistics: The significance of the differences between the groups was assessed by performing ANOVA followed by Tukey's test. A p value of less than 0.05 was considered

statistically significant. Data are presented as the mean ± standard error of the mean (SEM).

RESULTS

Characterization of transgene expression by MSCs: RT–PCR demonstrated RS1 expression in constitutive MSCs but not in untransfected AMSCs (Figure 1A). Similarly in inducible MSC *RS1* expression was present after induction with 100 ng/ml doxycycline (Figure 1B). Western blotting showed the presence of a 24 kDa RS1 protein in constitutive MSCs (Figure 1C) and after induction by doxycycline in the inducible MSCs (Figure 1D), as seen in the control Weri retinoblastoma cells. Using immunohistochemistry, the RS1 protein was localized to the cytoplasm in the constitutive MSCs and the inducible MSCs (Figure 1E). The amount of RS1 that was secreted into the extracellular media was compared to intracellular RS1 expression (Figure 1F). The constitutive and inducible MSCs secreted about the same amount of RS1 (about 8 ng/million cells/day), and they had similar intracellular amounts of RS1 (13.5 ng/million cells and 12 ng/million cells, respectively).

Topical doxycycline penetration to the posterior pole of the eye: To determine the optimal concentration of topical doxycycline for penetration into the vitreous cavity and the retina for in vivo studies, two different doses of doxycycline were tested (5 and 10 mg/ml). ELISA of the retinal lysates revealed that both doses of doxycycline gave the same lysate doxycycline concentrations of 3 ng/ml (Figure 2A). Therefore, we selected the lower dose of 5 mg/ml for the in vivo studies.

Single injection of RS1-expressing MSCs: After a single injection of either RS1-expressing constitutive MSCs or inducible MSCs into the vitreous cavity of the *Rs1h* KO mice, the amount of the RS1 protein in the retina was quantitated at 2, 4, or 8 weeks post-injection. No RS1 protein is present in the *Rs1h* KO mouse retina as previously reported (data not shown) [6]. The constitutive and inducible MSC treatments resulted in 10–12 pg/mg of the RS1 protein in retinal lysates at 2 weeks post-injection (Figure 2B). A gradual decline in RS1 expression was documented over time in both treatment groups. As expected, this decline correlated with previous observations that MSCs do not survive in the retinal microenvironment for more than 6–8 weeks [16].

The localization of RS1-expressing MSCs in the retina was detected using double immunolabeling with antibodies to PDGFRα (28) and RS1 (one) in the treated (constitutive MSCs and inducible MSCs) and untreated *Rs1h* eyes. Initially, 24 h post-injection, most of the MSCs were in the vitreous, with a few found on the internal limiting membrane (data not shown). At 8 weeks post-injection, RS1-expressing MSCs were detected in the inner nuclear layer (INL) of the retina with a gradient of RS1 staining (Figure 3A). Further away from the MSCs, the surrounding *Rs1h* retinal cells remained RS1-negative as would be expected compared to the wild-type cells, which showed high levels of RS1 expression in the inner segments and the INL of the retina (Figure 3B).

To determine whether injection of RS1-expressing MSCs had any structural effect on the *Rs1h* retina, histological sections were assessed. At 8 weeks post-injection, the INL appeared to be intact (Figure 3C) and comparable with the healthy mouse retina (Figure 3B) and differed from that in the untreated control group where schisis cavities were present in the INL (Figure 3C). To quantify the reduction in the schisis cavities, spidergrams were used to plot the size of the cavities in four quadrants of the retina (see the Methods section). The largest cavities were observed at the 2 week post-injection time point in all four quadrants (Figure 4A). Treated animals exhibited smaller schisis cavities in all four quadrants compared to the control groups. This was particularly evident in animals treated with inducible MSCs (Figure 4A). Smaller schisis cavities were also seen in eyes treated with genetically modified MSCs at later time points (Figures 4B,C). To assess the statistical significance of the differences in the schisis cavities seen in the different groups, the total schisis area from all four quadrants was compared at each time point. At 2 weeks post-injection, animals treated with either constitutive MSCs or inducible MSCs showed significantly smaller schisis areas (decreased by 65% and 83%, respectively) compared to the untreated ($p<0.0001$ for both) and vehicle groups ($p<0.001$ and $p<0.01$, respectively; Figure 4D). Similarly, at 4 weeks post injection, the constitutive MSC– and inducible MSC–treated groups had significantly smaller schisis areas than the untreated groups ($p<0.0001$ and $p<0.01$, respectively) and the vehicle groups ($p<0.01$ and $p<0.05$, respectively). At the 8-week time point, the untreated group had a significantly larger schisis area than the inducible MSC– and constitutive MSC–treated groups ($p<0.01$ and $p<0.05$, respectively). We also noted that delivery of unmodified AMSCs had some benefit on the extent of the schisis cavities although this did not reach statistical significance.

To determine whether the histological rescue we observed in the retina translated into functional benefits, ERG and OKT were performed. When measuring the scotopic b-/a-wave ratios of the ERG, a higher ratio indicates a better functional response. At all time points, the treated groups showed a higher ratio than the control groups (Figure 5A). At 4 weeks, the inducible MSC–treated group showed a significantly higher ratio than the untreated control group (2.6 versus 1.4, $p<0.05$). At the 8-week time point, the ratio for the

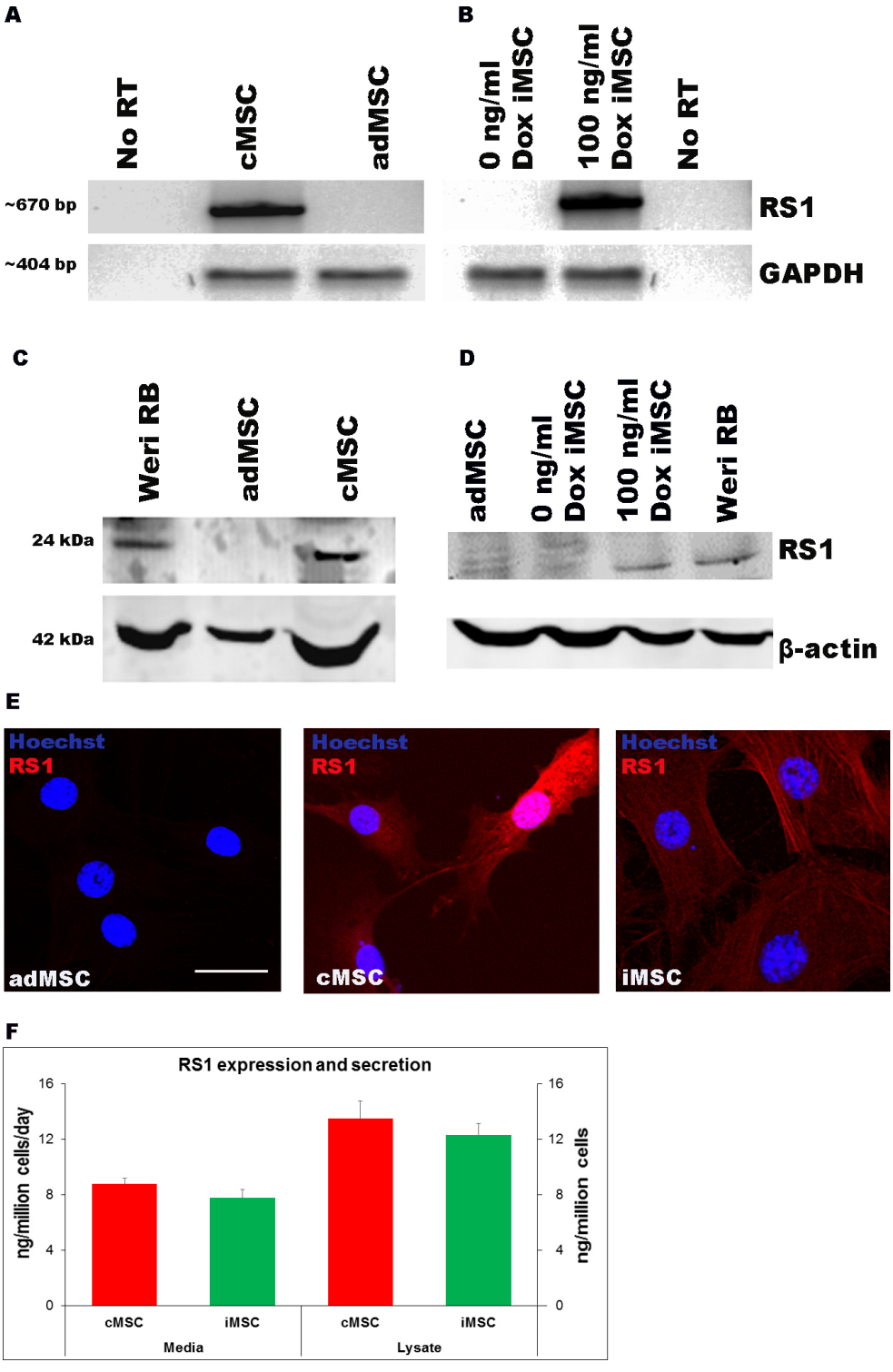

Figure 1. Expression and characterization of genetically modified MSCs. **A**: *RS1* mRNA expression (670 bp) in mesenchymal stem cells (MSCs) with a constitutive vector compared to the untransfected control cells (adipose tissue MSCs, AMSCs). No RT, without reverse transcriptase. GAPDH (404 bp) used as loading control. **B**: *RS1* mRNA expression in MSCs with the inducible vector (inducible MSCs). DOX = doxycycline. **C**: RS1 protein expression (24 kDa) in constitutive MSCs, untransfected AMSCs, and positive control Weri retinoblastoma (RB) cells. **D**: RS1 protein expression in MSCs with an inducible vector (inducible MSCs). Loading control, 42 kDa β-actin. **E**: Cytosolic RS1 localization (red) in constitutive MSCs and inducible MSCs, that is absent in untransfected AMSCs. Nuclei labeled with Hoechst (blue). **F**: Quantification of the rate of the RS1 protein secreted in the cell culture media and expressed by constitutive MSCs and inducible MSCs. Scale = 25 µm.

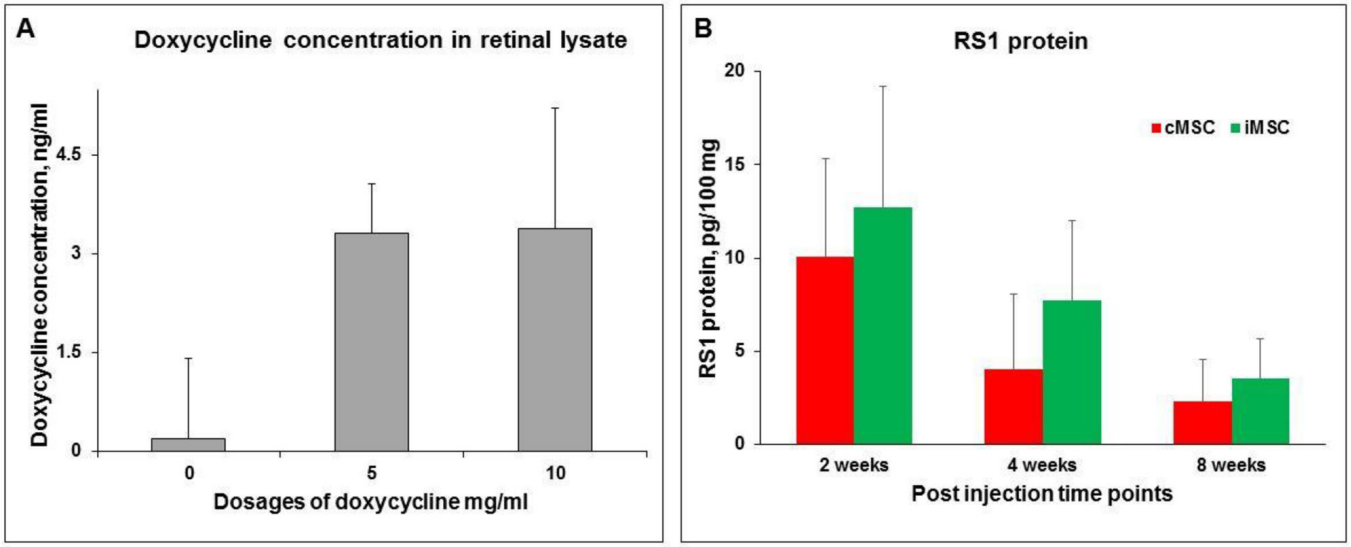

Figure 2. Doxycycline and RS1 concentration in the retina. **A**: Doxycycline concentration in retinal lysates after topical administration of either 5 mg/ml or 10 mg/ml doxycycline. **B**: Quantification of the amount of RS1 protein in retinal lysates after a single injection of RS1-expressing constitutive mesenchymal stem cells (MSCs) or inducible MSCs at three post-injection time points. All data are presented as mean ± standard error of the mean (SEM; n = 3).

eyes treated with inducible MSCs was significantly higher than that for all the other groups ($p<0.01$). These data suggest that the inducible RS1-expressing MSCs resulted in a better ERG response. The visual behavioral responses showed that at all time points the inducible MSC–treated animals demonstrated a higher spatial frequency threshold with a significant difference ($p<0.001$) at the 4-week time points, compared to the untreated mice (Figure 5B).

Multiple injections of RS1-expressing MSCs: After three injections of either RS1-expressing constitutive MSCs or inducible MSCs into the vitreous cavity of *Rs1h* mice, the amount of RS1 protein in the retina was quantitated at P120. The constitutive MSC and inducible MSC treatments resulted in approximately 7 pg/100 mg RS1 protein in retinal lysates (Figure 6A). This was two- to threefold higher than with the single injections of cells (2 pg/100 mg RS1 with constitutive MSCs and 3.75 pg/100 mg RS1 with inducible MSCs) at P77 (8 weeks; Figure 2B).

Immunohistochemistry revealed the presence of RS1-expressing MSCs in the inner retina of the treated mice compared to absence of the RS1 protein in the untreated control group (Figure 6B). In addition, the presence of schisis cavities appeared to be reduced (Figure 6C). Quantitation of the size of the schisis cavities was performed at P120 over an 800 µm area in the different treatment groups. Eyes treated with either constitutive MSCs or inducible MSCs had significantly smaller schisis areas (78% reduction) compared to the untreated control group ($p<0.01$, $p<0.05$, respectively; n = 6); however, there was no difference between the two treatment groups (Figure 7A). To assess the effect of RS1-expressing MSCs on the preservation of photoreceptor cells, the number of nuclei in the outer nuclear layer (ONL) over an 800 µm area was counted. There were significantly more nuclei in the constitutive MSC–treated group (62%, $p<0.0001$) and in the inducible MSC–treated group (87%, $p<0.0001$) compared to the control group (Figure 7B).

As it has been previously reported that the a- and b-waves of the scotopic ERG are decreased after P90 in the *Rs1h* mouse [26], both components were measured in the different treatment groups (Figure 7C). Treatment with either constitutive MSCs or inducible MSCs resulted in significantly increased a- and b-waves compared to the untreated control group ($p<0.05$, n = 6). Interestingly, the b-wave in the constitutive MSC treatment group was more than threefold higher than in the control group. This observation was also reflected in the optokinetic tracking responses that showed that constitutive MSC–treated animals had a significantly better spatial frequency threshold ($p<0.01$, n = 6) compared to the untreated control group (Figure 7D).

DISCUSSION

In this study, we investigated the feasibility of delivering the human RS1 protein to the *Rs1h* knockout mouse retina using MSCs that constitutively express RS1 or MSCs that

could be induced to express RS1 by exposure to doxycycline. We report that a single intravitreal injection of either type of RS1-expressing MSCs to the *Rs1h* knockout mouse eye achieves structural and functional benefits for up to 8 weeks post-injection. Furthermore, multiple monthly injections extended these benefits for up to 4 months. These data suggest that an ex vivo gene therapy approach could be feasible for treating patients with a mutation in the *RS1* gene in a postnatal clinical setting.

MSCs were selected as the cell of choice source in this study because of their ability to provide paracrine benefits, benefits established in preclinical studies in inherited retinal disease, and because of the ease with which they can be genetically modified ex vivo [29-33]. In this study, we also found that the unmodified MSC–treated groups showed minor structural benefits compared to the vehicle and untreated groups, though not at a statistically significant level. However, there were no significant functional or behavioral benefits. This might seem surprising as MSC therapy has been shown to be beneficial in other retinal dystrophies [34-36]. This may demonstrate the special circumstances of the pathophysiology of XLRS where the damaging structural effects of RS1 protein deficiency cannot be overcome by compensatory neuroprotective mechanisms [5]. Therefore, this study does not establish a likely benefit of combining paracrine effects with genetically-induced RS1 expression by using MSCs. Ultimately, a study that compares genetically modified MSCs with another genetically modified cell type would be needed to firmly establish this. Additionally, there have been reports that intravitreal MSC injection results in unacceptable preretinal fibrosis that is associated with poor graft integration [37]. However, recent work has suggested that this complication can be overcome to some extent by inhibiting the Janus kinase/signal transducers and activators of transcription (JAK/STAT3) signaling pathway [38]. Other benefits of the use of MSCs should also be kept in

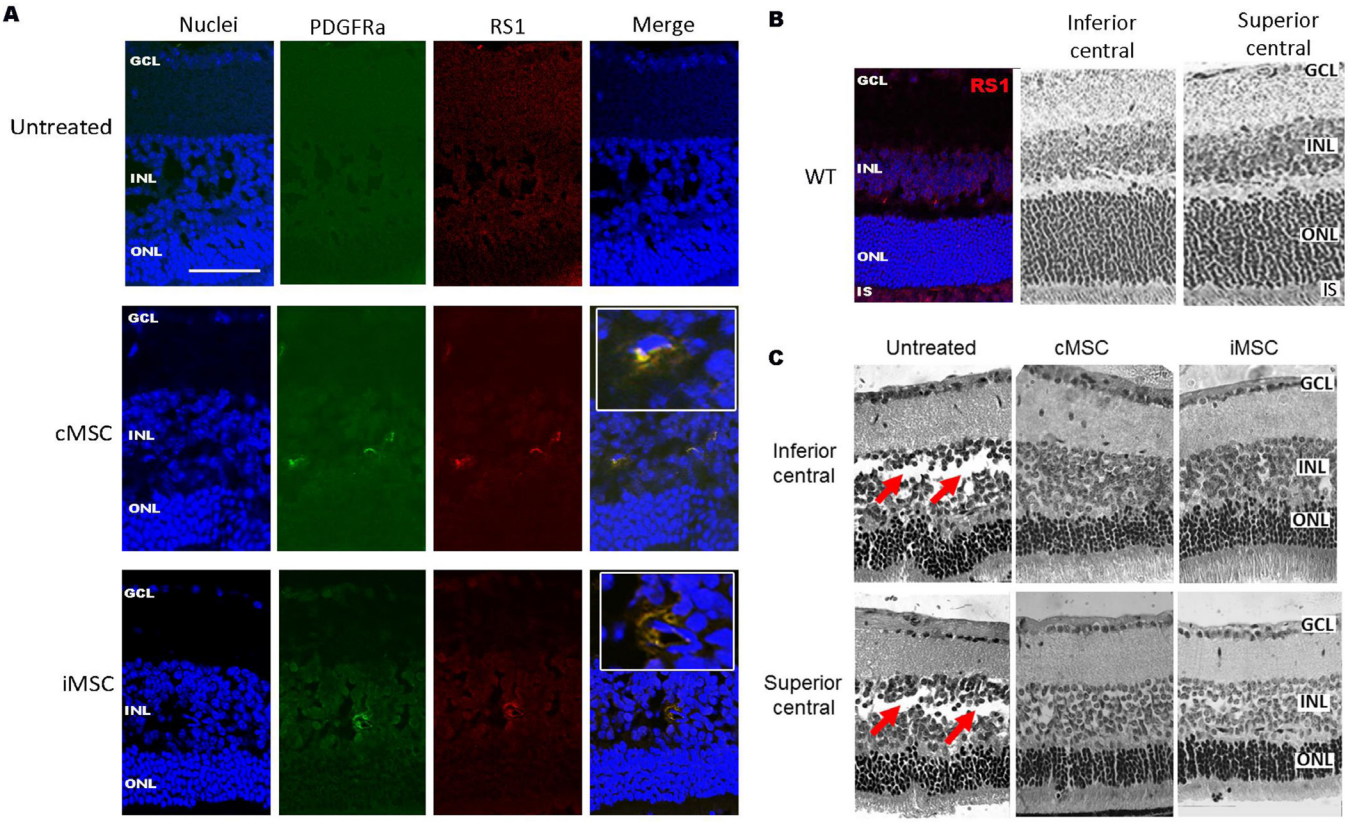

Figure 3. Single injection of RS1-expressing MSCs into the *Rs1h* mouse eye. **A**: Colocalization of RS1-expressing (red) and PDGFRα-expressing (green) constitutive mesenchymal stem cells (MSCs) and inducible MSCs at 8 weeks post-injection in the inner nuclear layer (INL), showing a gradient of fluorescent staining in the inset (3X higher magnification). GCL = ganglion cell layer; ONL = outer nuclear layer. **B**: Representative RS1 localization (red) and hematoxylin and eosin (H&E) staining of histology sections from the superior and inferior central quadrants of the wild-type retina. IS = inner segments. **C**: H&E staining of histology sections from the superior and inferior central quadrants of the retina in the inducible MSC and constitutive MSC-injected eyes compare to the untreated eye at 8 weeks post-injection. Scale bar = 50 µm.

mind, for example, ease of harvest, low immunogenicity [36], and safety for human clinical use, which is currently being explored in 389 clinical trials (including four studies in retinal degeneration) [https://clinicaltrials.gov/].

In any study where genetically modified, exogenous cells are injected into the eye, there is a risk of cells escaping the target site and expressing the therapeutic protein in other organs. It is also known that under certain conditions, MSCs can migrate and cross the blood–retinal barrier [15]. Theoretically then, MSCs constitutively expressing the RS1 protein could penetrate the blood vessels of the retina and lead to the expression of the RS1 protein in other organs with unknown consequences. To improve the safety of this ex vivo approach by anticipating such a scenario, we also studied the effectiveness of an inducible MSC cell line (in addition to the constitutively active constitutive MSC cell line) that would express RS1 only in tissues exposed to doxycycline. Although previous studies have used systemic induction of gene expression from MSCs injected into the eye [35,39,40], our results show for the first time that topical doxycycline can penetrate the retina and trigger secretion of the RS1 protein, demonstrating that a locally inducible ex vivo system is possible in the retina. The topical application of doxycycline to the eye significantly restricts doxycycline exposure in other organs and, thus, can prevent off-target effects of RS1 expression from inducible MSCs that might have made their way out of the eye. Interestingly, our results suggest that applying a higher concentration of topical doxycycline does not result in higher amounts of RS1 expression in vivo suggesting a plateau effect (Figure 2).

In previous studies, delivery of cell-based therapy to the retina used a sub-retinal injection technique. This has been in response to studies that show that the sub-retinal route results in migration of more cells in the photoreceptor layer [41]; however, sub-retinal delivery can be associated with significant local tissue damage [42]. Delivery by the intravitreal route has also been used. However, the ability of MSCs to penetrate the retina can be variable [34,43,44].

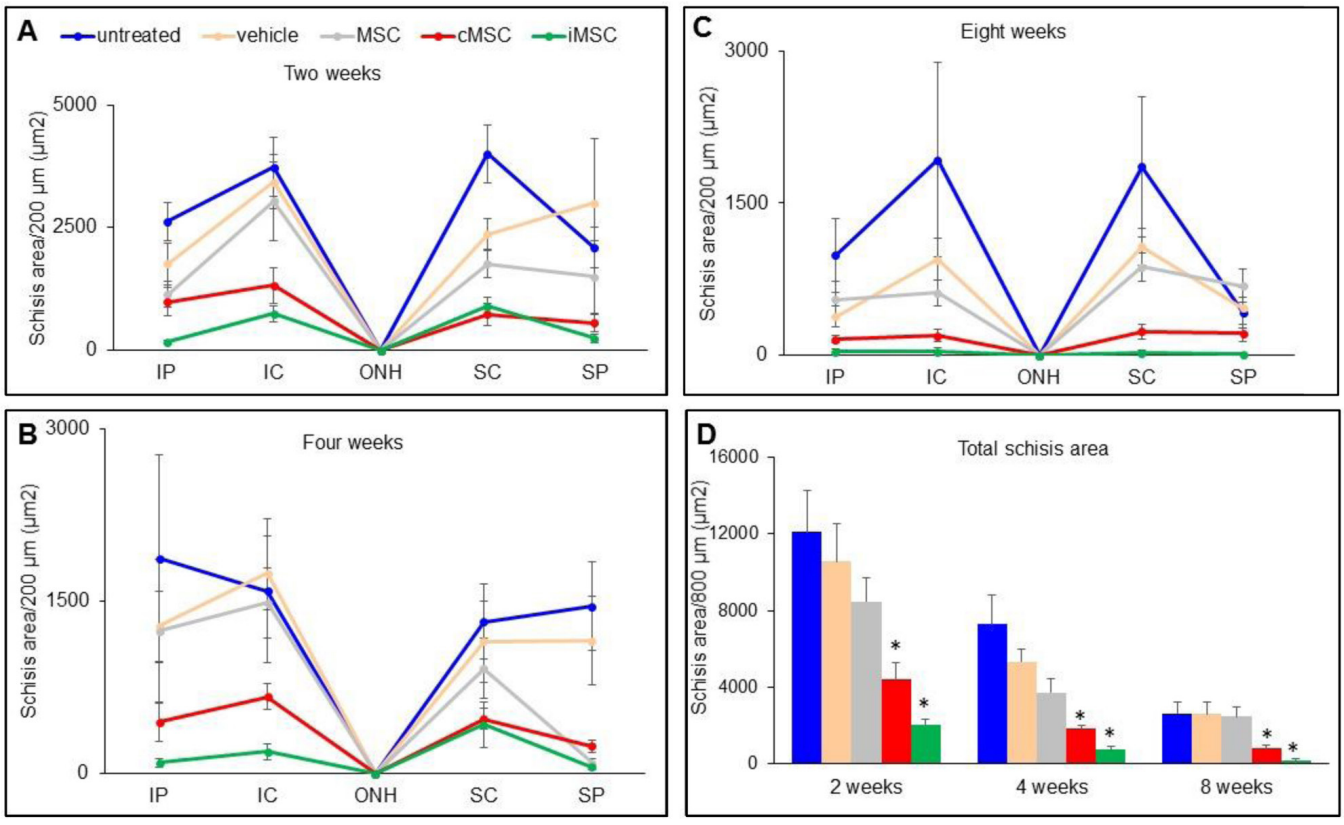

Figure 4. Schisis cavity measurements after injection of constitutive MSCs and inducible MSCs. **A**–**C**: Spidergrams of three post-injection time points comparing the schisis area in the four quadrants of the retina of the five different groups (untreated, vehicle-treated, untransfected mesenchymal stem cells [MSCs], constitutive MSCs, and inducible MSCs). **D**: The total schisis area from all four quadrants was calculated and compared among the groups at all three time points. Data are presented as mean ± standard error of the mean (SEM). IP = inferior peripheral; IC = inferior central; ONH = optic nerve head; SC = superior central; SP = superior peripheral. *p<0.05 (n = 6).

In this study, cells delivered intravitreally were able to reach the INL where RS1 is normally expressed, thus negating the need for sub-retinal delivery. Although MSCs were not seen to penetrate the ONL in large numbers, it could be assumed that since RS1 is secreted it would diffuse into deeper layers even if genetically modified MSCs were mainly restricted to the inner retina [22,45].

Two hallmark diagnostic features of human XLRS are an "electronegative ERG" and vitreoretinal dystrophy characterized by formation of cystic cavities in the inner retinal layers [46]. The knockout mouse model, used in this study, displays both phenotypes similar to human patients [22]. The negative ERG corresponds to a decrease in the b-wave amplitude with relative preservation of the a-wave in a scotopic ERG. This is mainly caused by defects in the synaptic transmission due to disorganized photoreceptor–bipolar synapse. To track functional rescue, the scotopic b-/a-wave ratio was measured for the single injection study, and we observed an increase in this ratio suggesting normalization of synaptic transmission to second-order neurons (e.g., bipolar and horizontal cells).

The structural and functional data indicated a better response from treatment with inducible MSCs than with constitutive MSCs. To better understand the reason behind this, we measured the amount of RS1 produced by these two lines in the retina. After a single injection and at all experimental time points, the inducible MSC–injected eyes were

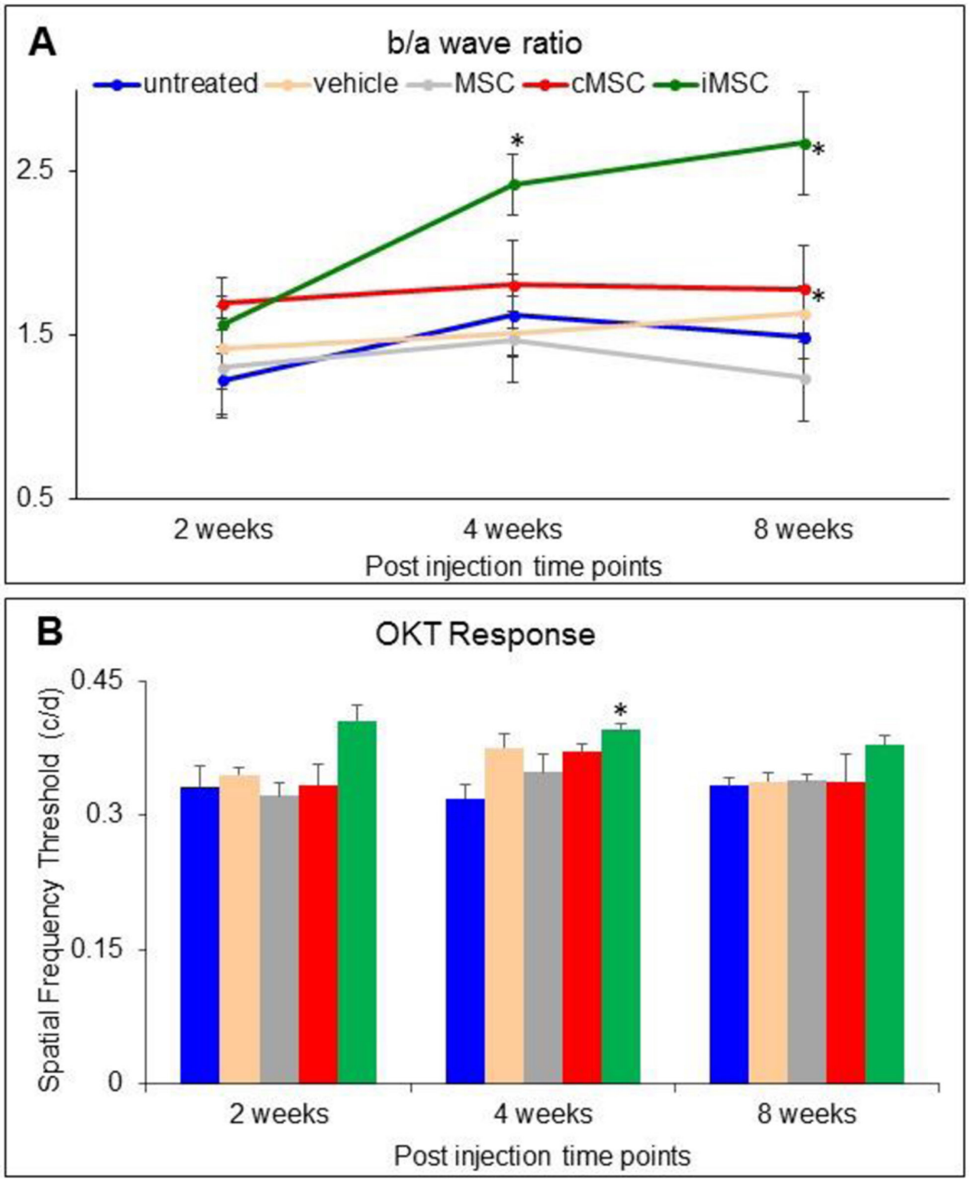

Figure 5. Functional and behavioral benefits of the RS1 therapy. **A**: The mean b-/a-wave ratio from the scotopic electroretinogram (ERG) were compared between treatment groups at 2, 4, and 8 weeks post-injection. **B**: The spatial frequency threshold was measured and compared between the groups at 2, 4 and 8 weeks post–injection. All data are presented as mean ± standard error of the mean (SEM; $p<0.05$, n=6).

found to have higher levels of RS1 expression, although the level did not reach statistical significance. This might be because there is a limit to the amount of RS1 protein that can be produced by the CMV promoter. In the case of the inducible cassette, it is controlled by the activation of the Tet response element (TRE) that is dependent on the amount of doxycycline in the system. The expression profile of RS1 by the two cell lines also reveals a declining pattern over time. The reason might be the reduction in the number of MSCs over time as it has been shown that MSCs survive in the eye for 6–8 weeks after intravitreal delivery [16]. The presence of doxycycline might have additionally contributed to the higher number of ONL cells and better a-wave response with multiple injections of inducible MSCs and long-term doxycycline use. A recent study showed that oral doxycycline monohydrate can improve some retinal function in patients with diabetic retinopathy, when compared to placebo [47]. However, a detailed mechanism of how doxycycline can improve the pathophysiology of retinal degeneration has yet to be described.

Three groups reported an in vivo gene therapy in the *Rs1h* knockout mouse model [6,7,9,22,48,49]. All used viral vectors, although the viral serotype, mode of injection, and promoter sequence were different. All reports showed structural benefits and functional rescue (normal b-wave) in the short- and long-term. As viral vectors were able to transfect a large number of cells from a single injection, RS1 expression was found from ganglion cells to the outer segment of the photoreceptors. More recently, in a targeted study, directing RS1 secretion specifically from photoreceptors with

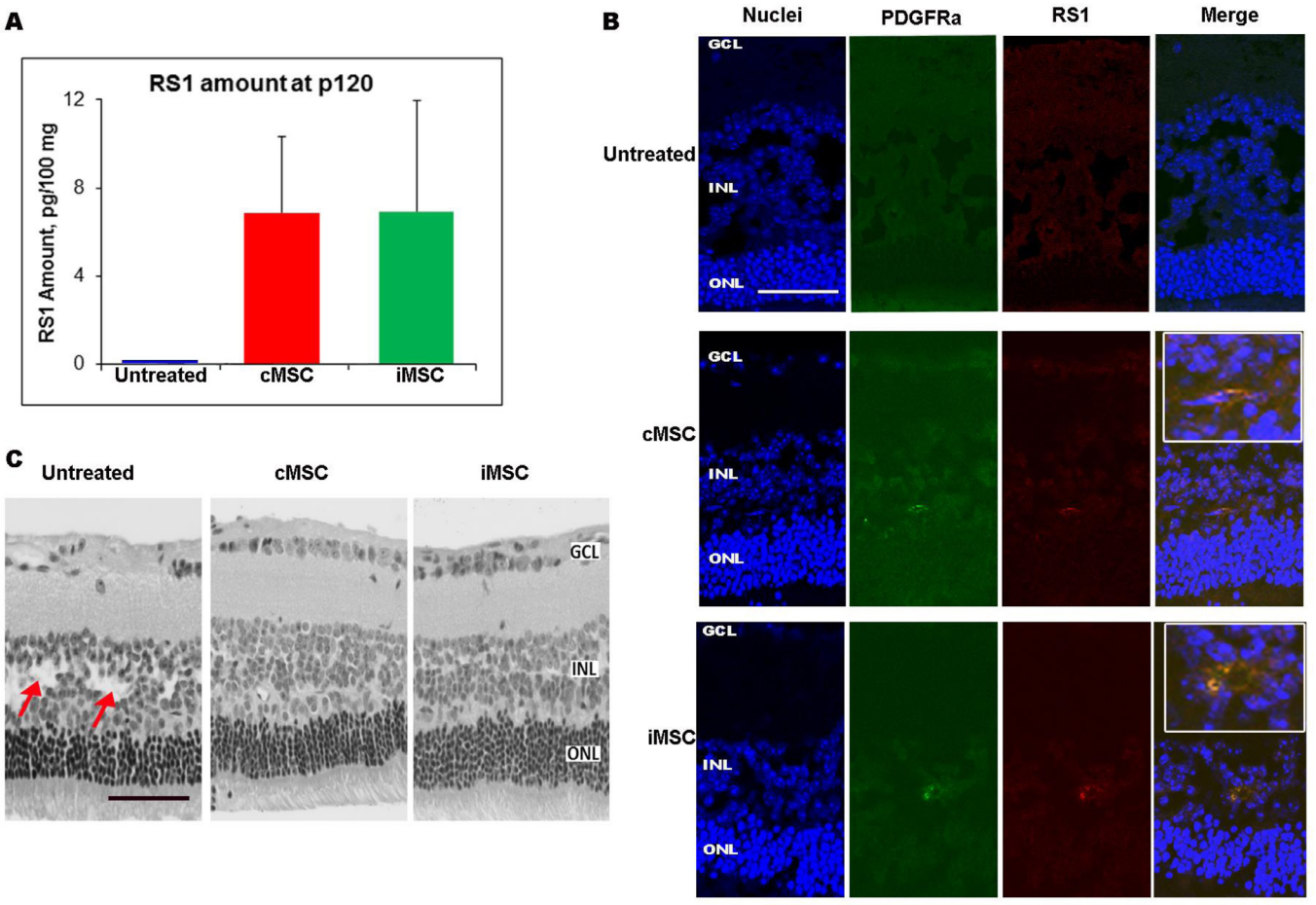

Figure 6. Quantitation and localization of RS1 in the retina after multiple injections. **A**: The amount of RS1 in retinal lysates at P120 was compared between the untreated group and the two treated groups. The mean of each group is presented with ± standard error of the mean (SEM). **B**: Representative immunohistochemical localization of the RS1 protein (red), colocalized with PDGFRα (green) expressing constitutive mesenchymal stem cells (MSCs) and inducible MSCs in treated versus untreated eyes at P120, showing a gradient of fluorescent staining in the inset (3X higher magnification). Nuclei are stained with Hoechst. **C**: Representative images of the inferior central quadrant of retina from each of the three groups. Schisis cavities indicated by arrows. Scale bar = 50 µm.

a rhodopsin promoter resulted in better in vivo functional responses compared to using a Müller cell–specific promoter [45]. This may be because retinoschisin is anchored to the surface of the photoreceptors through specific binding partners, including the Na/K-ATPase subunit ATP1A3, which is expressed in photoreceptors, but not in the Müller glia [50]. This lack of a binding partner in Müller cells might affect the stability or trafficking of retinoschisin to the photoreceptors. Interestingly, mesenchymal stem cells do express the ATP1A3 subunit [51], which may account for their ability to improve the retinal architecture in the *Rsh1* mouse. However, one potential problem is that the disease models in these studies were not completely comparable to the human condition, as the mice were knockout models with no retinoschisin protein expression, whereas some human patients express a mutant protein that may interfere with the endogenously expressed retinoschisin. Two studies have shown that for some of the most commonly occurring disease mutations, exogenous wild-type RS1 secretion was not affected by the ectopic expression of the mutant protein [52,53]. However, some of the mutated form of RS1 coassembled with the wild-type polypeptide and failed to secrete from the cell. This type of retention and accumulation could lead to stress in the cell [53]. Highly metabolically active cells, such as photoreceptors might also behave in a different way in response to the accumulated protein than the cell lines that were used in these studies. Moreover, a recent study showed that a neutralizing factor against adenoassociated virus (AAV) vectors could be present in the vitreous [54], which could limit the efficiency of in vivo gene therapy making an ex vivo strategy more attractive. Such an ex vivo approach also has inherent limitations. For instance, to maintain a steady and therapeutically relevant amount of the RS1 protein, repeated injections are required. Multiple intraocular injections could potentially increase the chance of collateral damage in the eye. A systemic delivery of the cells with a targeting mechanism to the eye could help reduce that risk [16].

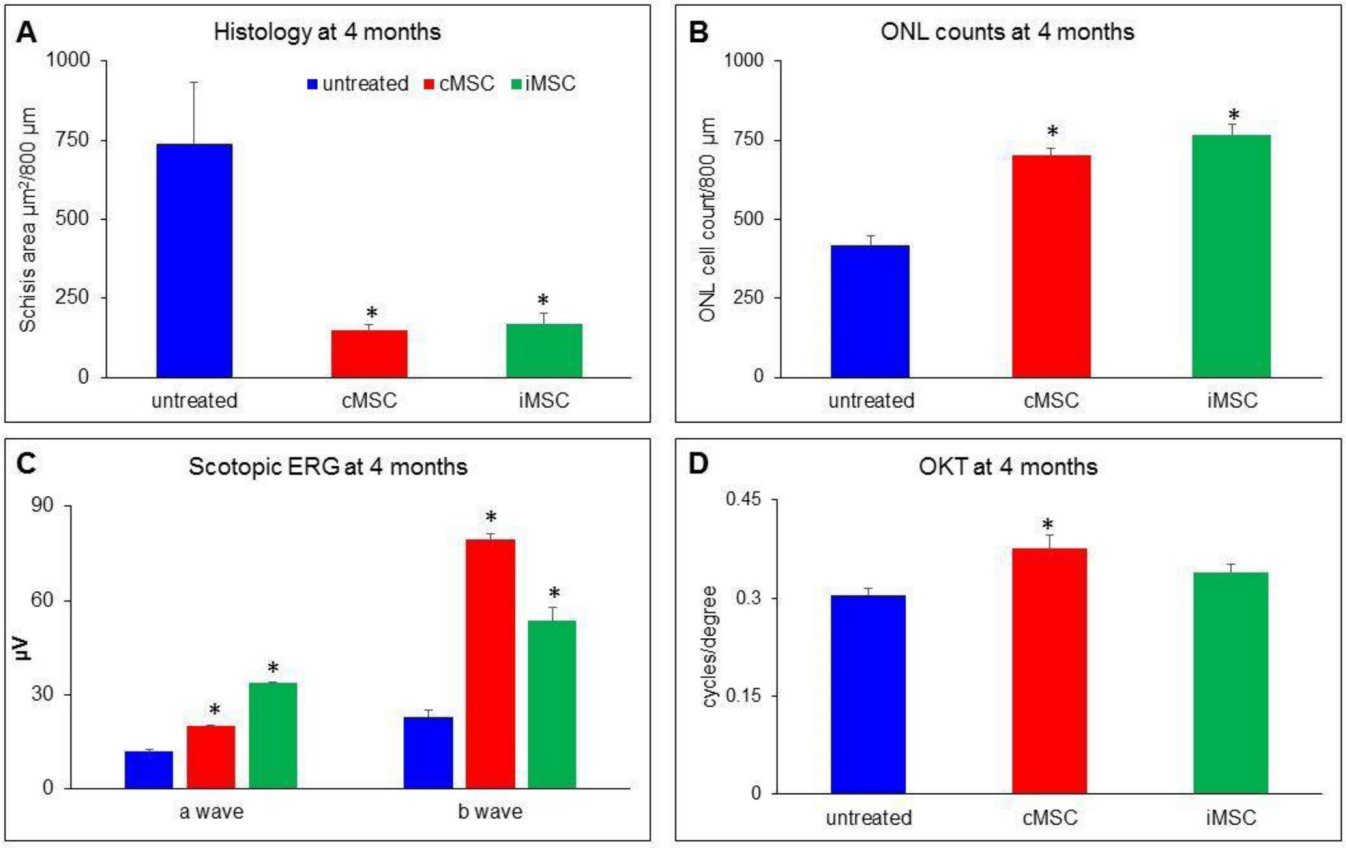

Figure 7. Assessment of multiple injections of RS1-expressing MSCs at P120. **A**: The total schisis areas from four quadrants were calculated and compared among three groups. **B**: Number of photoreceptor nuclei in the outer nuclear layer (ONL). **C**: A- and b-wave measurements from scotopic electroretinogram (ERG). **D**: Spatial frequency thresholds (cycles per degree) in the different treatment groups. Data are presented as the mean ± standard error of the mean (SEM; *, $p<0.05$, $n = 6$).

This proof-of-principle suggests that this inducible ex vivo approach can also be applied to other similar ocular disorders where deficiency of a functional, extracellular protein is the major cause of the disease. Sorsby's fundus dystrophy is one such disease where the non-functional tissue inhibitor of metalloproteinases 3 (TIMP3) could disrupt the controlled degradation of the extracellular matrix (ECM) around the blood vessels in the retina [55]. Lack of TIMP3 leads to excessive degradation of the ECM and retinal neovascularization. Sub-retinal delivery of genetically modified MSCs expressing TIMP3 protein has the potential to reverse the disease condition. Other multifactorial diseases could potentially be targeted with the inducible ex vivo approach. For example, it has been reported that doxycycline-inducible expression of erythropoietin from rat MSCs can protect and rescue the RPE and retinal neurons after sodium iodide–induced age-related macular degeneration (AMD)-like retinal degenerations [35]. Another option might be to deliver MSCs that secrete proteolytic enzymes that could break down retinal drusen. Finally, ex vivo delivery of extracellular matrix proteins would be advantageous in diseases where the transcript size is too large for viral vector gene therapy, for example, FBN2 in macular dystrophy [56] and IMPG2 in retinitis pigmentosa [57], which have transcripts of 9.3 Kb and 8.3 Kb, respectively. In summary, this study demonstrates that a mesenchymal stem cell–based ex vivo gene therapy approach for treatment of X-linked retinoschisis is a feasible strategy that could now be tested in the clinical setting.

ACKNOWLEDGMENTS

We thank Dr. Robert Molday (UBC) for providing the *Rs1h* knockout mouse model, the human *RS1* cDNA, and RS1 polyclonal antibody; and Dr. Xia Wang (UBC) for providing the wild-type mice. This work was supported by a Team Grant (to KGE/CGE) from the Canadian Institutes of Health Research (#222728). The authors declare no conflict of interest.

REFERENCES

1. Molday LL, Hicks D, Sauer CG, Weber BH, Molday RS. Expression of X-linked retinoschisis protein RS1 in photoreceptor and bipolar cells. Invest Ophthalmol Vis Sci 2001; 42:816-25. [PMID: 11222545].
2. Sauer CG, Gehrig A, Warneke-Wittstock R, Marquardt A, Ewing CC, Gibson A, Lorenz B, Jurklies B, Weber BH. Positional cloning of the gene associated with X-linked juvenile retinoschisis. Nat Genet 1997; 17:164-70. [PMID: 9326935].
3. . The Retinoschisis Consortium. Functional implications of the spectrum of mutations found in 234 cases with X-linked juvenile retinoschisis. Hum Mol Genet 1998; 7:1185-92. [PMID: 9618178].
4. Sergeev YV, Vitale S, Sieving PA, Vincent A, Robson AG, Moore AT, Webster AR, Holder GE. Molecular modeling of retinoschisin with functional analysis of pathogenic mutations from human X-linked retinoschisis. Hum Mol Genet 2010; 19:1302-13. [PMID: 20061330].
5. Molday RS, Kellner U, Weber BH. X-linked juvenile retinoschisis: clinical diagnosis, genetic analysis, and molecular mechanisms. Prog Retin Eye Res 2012; 31:195-212. [PMID: 22245536].
6. Kjellstrom S, Bush RA, Zeng Y, Takada Y, Sieving PA. Retinoschisin gene therapy and natural history in the Rs1h-KO mouse: long-term rescue from retinal degeneration. Invest Ophthalmol Vis Sci 2007; 48:3837-45. [PMID: 17652759].
7. Janssen A, Min SH, Molday LL, Tanimoto N, Seeliger MW, Hauswirth WW, Molday RS, Weber BH. Effect of late-stage therapy on disease progression in AAV-mediated rescue of photoreceptor cells in the retinoschisin-deficient mouse. Mol Ther 2008; 16:1010-7. [PMID: 18388913].
8. Takada Y, Vijayasarathy C, Zeng Y, Kjellstrom S, Bush RA, Sieving PA. Synaptic pathology in retinoschisis knockout (Rs1-/y) mouse retina and modification by rAAV-Rs1 gene delivery. Invest Ophthalmol Vis Sci 2008; 49:3677-86. [PMID: 18660429].
9. Park TK, Wu Z, Kjellstrom S, Zeng Y, Bush RA, Sieving PA, Colosi P. Intravitreal delivery of AAV8 retinoschisin results in cell type-specific gene expression and retinal rescue in the Rs1-KO mouse. Gene Ther 2009; 16:916-26. [PMID: 19458650].
10. McCormack MP, Rabbitts TH. Activation of the T-cell oncogene LMO2 after gene therapy for X-linked severe combined immunodeficiency. N Engl J Med 2004; 350:913-22. [PMID: 14985489].
11. Kaiser J. Clinical trials. Gene transfer an unlikely contributor to patient's death. Science 2007; 318:1535-[PMID: 18063761].
12. Smith RH. Adeno-associated virus integration: virus versus vector. Gene Ther 2008; 15:817-22. [PMID: 18401436].
13. Bushman FD. Retroviral integration and human gene therapy. J Clin Invest 2007; 117:2083-6. [PMID: 17671645].
14. Bashar AE, Metcalfe A, Yanai A, Laver C, Häfeli UO, Gregory-Evans CY, Moritz OL, Matsubara JA, Gregory-Evans K. Influence of iron oxide nanoparticles on innate and genetically modified secretion profiles of mesenchymal stem cells. IEEE Trans Magn 2013; 49:389-93. [PMID: 24976643].
15. Joe AW, Gregory-Evans K. Mesenchymal stem cells and potential applications in treating ocular disease. Curr Eye Res 2010; 35:941-52. [PMID: 20958182].
16. Yanai A, Häfeli UO, Metcalfe AL, Soema P, Addo L, Gregory-Evans CY, Po K, Shan X, Moritz OL, Gregory-Evans K. Focused magnetic stem cell targeting to the retina using superparamagnetic iron oxide nanoparticles. Cell Transplant 2012; 21:1137-48. [PMID: 22405427].

17. Tracy CJ, Sanders DN, Bryan JN, Jensen CA, Castaner LJ, Kirk MD, Katz ML. Intravitreal implantation of genetically modified autologous bone marrow-derived stem cells for treating retinal disorders. Adv Exp Med Biol 2016; 854:571-7. [PMID: 26427461].

18. Roubeix C, Godefroy D, Mias C, Sapienza A, Riancho L, Degardin J, Fradot V, Ivkovic I, Picaud S, Sennlaub F, Denoyer A, Rostene W, Sahel JA, Parsadaniantz SM. Brignole- Baudouin F, Baudouin C. Intraocular pressure reduction and neuroprotection conferred by bone marrow-derived mesenchymal stem cells in an animal model of glaucoma. Stem Cell Res Ther 2015; 6:177-[PMID: 26377305].

19. Tzameret A, Sher I, Belkin M, Treves AJ, Meir A, Nagler A, Levkovitch-Verbin H, Rotenstreich Y, Solomon AS. Epiretinal transplantation of human bone marrow mesenchymal stem cells rescues retinal and vision function in a rat model of retinal degeneration. Stem Cell Res (Amst) 2015; 15:387-94. [PMID: 26322852].

20. Leow SN, Luu CD, Hairul Nizam MH, Mok PL, Ruhaslizan R, Wong HS, Wan Abdul Halim WH, Ng MH, Ruszymah BH, Chowdhury SR, Bastion ML, Then KY. Safety and efficacy of human Wharton's jelly-derived mesenchymal stem cells therapy for retinal degeneration. PLoS One 2015; 10:e0128973-[PMID: 26107378].

21. Gossen M, Bujard H. Tight control of gene expression in mammalian cells by tetracycline responsive promoters. Proc Natl Acad Sci USA 1992; 89:5547-51. [PMID: 1319065].

22. Min SH, Molday LL, Seeliger MW, Dinculescu A, Timmers AM, Janssen A, Tonagel F, Tanimoto N, Weber BH, Molday RS, Hauswirth WW. Prolonged recovery of retinal structure/function after gene therapy in an Rs1h-deficient mouse model of x–linked juvenile retinoschisis. Mol Ther 2005; 12:644-51. [PMID: 16027044].

23. Grayson C, Reid SN, Ellis JA, Rutherford A, Sowden JC, Yates JR, Farber DB, Trump D. Retinoschisin, the X-linked retinoschisis protein, is a secreted photoreceptor protein, and is expressed and released by Weri-Rb1 cells. Hum Mol Genet 2000; 9:1873-9. [PMID: 10915776].

24. Douglas RM, Alam NM, Silver BD, McGill TJ, Tschetter WW, Prusky GT. Independent visual threshold measurements in the two eyes of freely moving rats and mice using a virtual-reality optokinetic system. Vis Neurosci 2005; 22:677-84. [PMID: 16332278].

25. Gregory-Evans K, Po K, Chang F, Gregory-Evans CY. Pharmacological enhancement of ex vivo gene therapy neuroprotection in a rodent model of retinal degeneration. Ophthalmic Res 2012; 47:32-8. [PMID: 21691141].

26. Weber BH, Schrewe H, Molday LL, Gehrig A, White KL, Seeliger MW, Jaissle GB, Friedburg C, Tamm E, Molday RS. Inactivation of the murine X-linked juvenile retinoschisis gene, Rs1h, suggests a role of retinoschisin in retinal cell layer organization and synaptic structure. Proc Natl Acad Sci USA 2002; 99:6222-7. [PMID: 11983912].

27. Lin CS, Xin ZC, Dai J, Lue TF. Commonly used mesenchymal stem cell markers and tracking labels: Limitations and challenges. Histol Histopathol 2013; 28:1109-16. [PMID: 23588700].

28. Farahani RM, Xaymardan M. Platelet-derived growth factor receptor alpha as a marker of mesenchymal stem cells in development and stem cell biology. Stem Cells Int 2015; xxx:362753-.

29. Rodriguez-Crespo D, Di Lauro S, Singh AK, Garcia-Gutierrez MT, Garrosa M, Pastor JC, Fernandez-Bueno I, Srivastava GK. Triple-layered mixed co-culture model of RPE cells with neuroretina for evaluating the neuroprotective effects of adipose-MSCs. Cell Tissue Res 2014; 358:705-16. [PMID: 25213807].

30. Ahn SY, Chang YS, Park WS. Mesenchymal stem cells transplantation for neuroprotection in preterm infants with severe intraventricular hemorrhage. Korean J Pediatr 2014; 57:251-6. [PMID: 25076969].

31. Jiang Y, Zhang Y, Zhang L, Wang M, Zhang X, Li X. Therapeutic effect of bone marrow mesenchymal stem cells on laser-induced retinal injury in mice. Int J Mol Sci 2014; 15:9372-85. [PMID: 24871366].

32. Yan Y, Ma T, Gong K, Ao Q, Zhang X, Gong Y. Adipose-derived mesenchymal stem cell transplantation promotes adult neurogenesis in the brains of Alzheimer's disease mice. Neural Regen Res 2014; 9:798-805. [PMID: 25206892].

33. Anbari F, Khalili MA, Bahrami AR, Khoradmehr A, Sadeghian F, Fesahat F, Nabi A. Intravenous transplantation of bone marrow mesenchymal stem cells promotes neural regeneration after traumatic brain injury. Neural Regen Res 2014; 9:919-23. [PMID: 25206912].

34. Johnson TV, Bull ND, Hunt DP, Marina N, Tomarev SI, Martin KR. Neuroprotective effects of intravitreal mesenchymal stem cell transplantation in experimental glaucoma. Invest Ophthalmol Vis Sci 2010; 51:2051-9. [PMID: 19933193].

35. Guan Y, Cui L, Qu Z, Lu L, Wang F, Wu Y, Zhang J, Gao F, Tian H, Xu L, Xu G, Li W, Jin Y, Xu GT. Subretinal transplantation of rat MSCs and erythropoietin gene modified rat MSCs for protecting and rescuing degenerative retina in rats. Curr Mol Med 2013; 13:1419-31. [PMID: 23971737].

36. Yang Z, Li K, Yan X, Dong F, Zhao C. Amelioration of diabetic retinopathy by engrafted human adipose-derived mesenchymal stem cells in streptozotocin diabetic rats. Graefes Arch Clin Exp Ophthalmol •••; 201:1415-22. [PMID: 20437245].

37. Johnson TV, Bull ND, Martin KR. Identification of barriers to retinal engraftment of transplanted stem cells. Invest Ophthalmol Vis Sci 2010; 51:960-70. [PMID: 19850833].

38. Tassoni A, Gutteridge A, Barber AC, Osborne A, Martin KR. Molecular mechanisms mediating retinal reactive gliosis following bone marrow mesenchymal stem cell transplantation. Stem Cells 2015; 33:3006-16. [PMID: 26175331].

39. Mi XS, Zhang X, Feng Q, Lo AC, Chung SK, So KF. Progressive retinal degeneration in transgenic mice with overexpression of endothelin-1 in vascular endothelial cells. Invest Ophthalmol Vis Sci 2012; 53:4842-51. [PMID: 22729434].

40. Yuan Y, Yeh LK, Liu H, Yamanaka O, Hardie WD, Kao WW, Liu CY. Targeted overexpression of TGF-alpha in the corneal epithelium of adult transgenic mice induces changes in anterior segment morphology and activates noncanonical Wnt signaling. Invest Ophthalmol Vis Sci 2013; 54:1829-37. [PMID: 23412089].

41. Huo DM, Dong FT, Yu WH, Gao F. Differentiation of mesenchymal stem cell in the microenviroment of retinitis pigmentosa. Int J Ophthalmol 2010; 3:216-9. [PMID: 22553557].

42. Laver CR, Metcalfe AL, Szczygiel L, Yanai A, Sarunic MV, Gregory-Evans K. Bimodal in vivo imaging provides early assessment of stem-cell-based photoreceptor engraftment. Eye (Lond) 2015; 29:681-90. [PMID: 25771816].

43. Machalinska A, Kawa M, Pius-Sadowska E, Stępniewski J, Nowak W, Rogińska D, Kaczyńska K, Baumert B, Wiszniewska B, Józkowicz A, Dulak J, Machaliński B. Long-term neuroprotective effects of NT-4-engineered mesenchymal stem cells injected intravitreally in a mouse model of acute retinal injury. Invest Ophthalmol Vis Sci 2013; 54:8292-305. [PMID: 24265016].

44. Haddad-Mashadrizeh A, Bahrami AR, Matin MM, Edalatmanesh MA, Zomorodipour A, Gardaneh M, Farshchian M, Momeni-Moghaddam M. Human adipose-derived mesenchymal stem cells can survive and integrate into the adult rat eye following xenotransplantation. Xenotransplantation 2013; 20:165-76. [PMID: 23679842].

45. Byrne LC, Oztürk BE, Lee T, Fortuny C, Visel M, Dalkara D, Schaffer DV, Flannery JG. Retinoschisin gene therapy in photoreceptors, Muller glia or all retinal cells in the Rs1h−/− mouse. Gene Ther 2014; 21:585-92. [PMID: 24694538].

46. Vijayasarathy C, Ziccardi L, Sieving PA. Biology of retinoschisin. Adv Exp Med Biol 2012; 723:513-8. [PMID: 22183371].

47. Scott IU, Jackson GR, Quillen DA, Klein R, Liao J, Gardner TW. Effect of doxycycline vs placebo on retinal function and diabetic retinopathy progression in patients with severe nonproliferative or non-high-risk proliferative diabetic retinopathy: a randomized clinical trial. JAMA Ophthalmol 2014; 132:535-43. [PMID: 24604308].

48. Zeng Y, Takada Y, Kjellstrom S, Hiriyanna K, Tanikawa A, Wawrousek E, Smaoui N, Caruso R, Bush RA, Sieving PA. RS-1 gene delivery to an adult Rs1h knockout mouse model restores ERG b-wave with reversal of the electronegative waveform of X-linked retinoschisis. Invest Ophthalmol Vis Sci 2004; 45:3279-85. [PMID: 15326152].

49. Apaolaza PS, Del Pozo-Rodríguez A, Torrecilla J, Rodríguez-Gascón A, Rodríguez JM, Friedrich U, Weber BH, Solinís MA. Solid lipid nanoparticle-based vectors intended for the treatment of X-linked juvenile retinoschisis by gene therapy: In vivo approaches in Rs1hdeficient mouse model. J Control Release 2015; 217:273-83. [PMID: 26400864].

50. Molday LL, Wu WW, Molday RS. Retinoschisin (RS1), the protein encoded by the X-linked retinoschisis gene, is anchored to the surface of retinal photoreceptor and bipolar cells through its interactions with a Na/K ATPase-SARM1 complex. J Biol Chem 2007; 282:32792-801. [PMID: 17804407].

51. Yu W, Qian C, Jiang X, Weng W. Mechanisms of stem cell osteogenic differentiation on TiO2 nanotubes. Colloids Surf B Biointerfaces 2015; 136:779-85. [PMID: 26520050].

52. Dyka FM, Molday RS. Coexpression and interaction of wild-type and missense RS1 mutants associated with X-linked retinoschisis: its relevance to gene therapy. Invest Ophthalmol Vis Sci 2007; 48:2491-7. [PMID: 17525175].

53. Gleghorn LJ, Trump D, Bulleid NJ. Wild-type and missense mutants of retinoschisin coassemble resulting in either intracellular retention or incorrect assembly of the functionally active octamer. Biochem J 2010; 425:275-83. [PMID: 19849666].

54. Cheng Y, Huang L, Li X, Qi H, Zhou P, Yu W, Jiang YA, Wadsworth S, Scaria A. Prevalence of neutralizing factors against adeno-associated virus types 2 in age-related macular degeneration and polypoidal choroidal vasculopathy. Curr Gene Ther 2013; 13:182-8. [PMID: 23590636].

55. Pescosolido N, Barbato A, Pascarella A, Giannotti R, Genzano M, Nebbioso M. Role of protease-inhibitors in ocular diseases. Molecules 2014; 19:20557-69. [PMID: 25493637].

56. Ratnapriya R, Zhan X, Fariss RN, Branham KE, Zipprer D, Chakarova CF, Sergeev YV, Campos MM, Othman M, Friedman JS, Maminishkis A, Waseem NH, Brooks M, Rajasimha HK, Edwards AO, Lotery A, Klein BE, Truitt BJ, Li B, Schaumberg DA, Morgan DJ, Morrison MA, Souied E, Tsironi EE, Grassmann F, Fishman GA, Silvestri G, Scholl HP, Kim IK, Ramke J, Tuo J, Merriam JE, Merriam JC, Park KH, Olson LM, Farrer LA, Johnson MP, Peachey NS, Lathrop M, Baron RV, Igo RP Jr, Klein R, Hagstrom SA, Kamatani Y, Martin TM, Jiang Y, Conley Y, Sahel JA, Zack DJ, Chan CC, Pericak-Vance MA, Jacobson SG, Gorin MB, Klein ML, Allikmets R, Iyengar SK, Weber BH, Haines JL, Léveillard T, Deangelis MM, Stambolian D, Weeks DE, Bhattacharya SS, Chew EY, Heckenlively JR, Abecasis GR, Swaroop A. Rare and common variants in extracellular matrix gene Fibrillin 2 (FBN2) are associated with macular degeneration. Hum Mol Genet 2014; 23:5827-37. [PMID: 24899048].

57. Bandah-Rozenfeld D, Collin RW, Banin E, van den Born LI, Coene KL, Siemiatkowska AM, Zelinger L, Khan MI, Lefeber DJ, Erdinest I, Testa F, Simonelli F, Voesenek K, Blokland EA, Strom TM, Klaver CC, Qamar R, Banfi S, Cremers FP, Sharon D, den Hollander AI. Mutations in IMPG2, encoding interphotoreceptor matrix proteoglycan 2, cause autosomal-recessive retinitis pigmentosa. Am J Hum Genet 2010; 87:199-208. [PMID: 20673862].

Articles are provided courtesy of Emory University and the Zhongshan Ophthalmic Center, Sun Yat-sen University, P.R. China. The print version of this article was created on 24 June 2016. This reflects all typographical corrections and errata to the article through that date. Details of any changes may be found in the online version of the article.